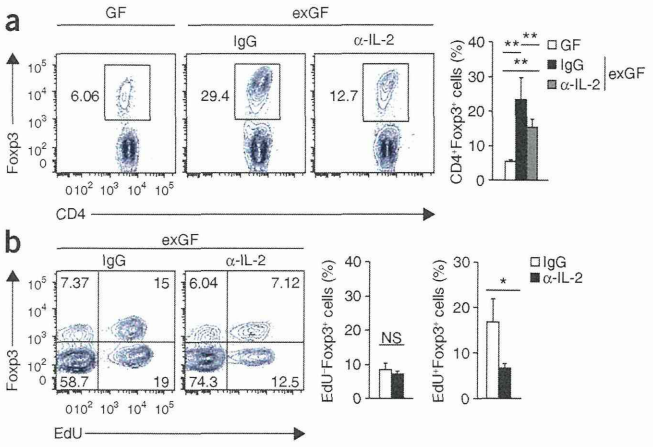

Figure 2 IL-2 is responsible for the vigorous proliferation of colonic T_{reg} cells after inoculation of commensal bacteria. (**a**) Foxp3 expression by $CD4^+$ T cells in the cLP of GF mice left untreated and exGF mice inoculated with bacteria (as in **Fig. 1a**) and, 3 d later, given intravenous injection of control IgG or IL-2-neutralizing antibody (α-IL-2) and assessed 2 d later. Numbers adjacent to outlined areas (left) indicate percent $Foxp3^+CD4^+$ T cells. (**b**) Proliferation of $CD4^+$ T cells in the cLP of exGF mice treated as in **a**. Numbers in quadrants (left) indicate percent cells in each. $^*P < 0.05$ and $^{**}P < 0.01$ (one-way analysis of variance (ANOVA) followed by Tukey's test (**a**) or Student's *t*-test (**b**)). Data are representative of at least three independent experiments (error bars, s.d. of three mice).

T_{reg} cells with neutralizing antibodies to integrin $\alpha_4\beta_7$ subunits[11] before administering the thymidine analog EdU to exGF mice. This treatment affected the abundance of proliferative T_{reg} cells in the colon only marginally (**Fig. 1d**). Collectively, these results suggested that colonization by commensal bacteria induced extensive proliferation of T_{reg} cells mainly in the colonic mucosa.

IL-2 is responsible for colonic T_{reg} cell population expansion

IL-2, which is well documented as promoting the proliferation of T_{reg} cells[22], was induced in the colonic mucosa, particularly in $CD4^+$ T cells after inoculation of mice with bacteria (**Fig. 1a**). Similarly, colonic $CD4^+$ T cells of infant mice (around 2 weeks old) housed in SPF conditions had high expression of IL-2; during this time, T_{reg} cells displayed active proliferation in the cLP but not in the spleen (**Supplementary Fig. 1b,d**). We therefore postulated that early induction of IL-2 may have been responsible for the local proliferation of T_{reg} cells. To test this idea, we treated exGF mice with neutralizing antibody to IL-2. As expected, abrogation of IL-2 strongly suppressed the induction of colonic T_{reg} cells (**Fig. 2a**). There was also a significantly lower abundance of EdU^+ proliferating T_{reg} cells in the antibody-treated exGF mice than in their counterparts treated with the control antibody immunoglobulin G (IgG) (**Fig. 2b**). On the basis of these observations, we reasoned that an early IL-2 response was indispensable for the proliferation of T_{reg} cells in the colon.

IL-2 upregulates *Uhrf1* in colonic T_{reg} cells

We explored the molecular machinery that mediates the proliferation of colonic T_{reg} cells. First we profiled genes selectively upregulated in T_{reg} cells from exGF mice (**Fig. 3a**, cluster I). We also categorized IL-2-responsive genes (**Fig. 3b**, cluster II). After comparison of the two clusters, followed by gene ontology–based functional analysis, we selected several candidate genes encoding molecules potentially associated with the proliferation of colonic T_{reg} cells in an IL-2-dependent manner (**Fig. 3c**). Among those specifically upregulated in colonic T_{reg} cells was *Uhrf1* (**Fig. 3d**). *Uhrf1* expression was highest in T_{reg} cells among colonic $CD4^+$ T cell subsets in SPF mice (**Fig. 3e**). We confirmed that IL-2 was essential for *Uhrf1* expression by colonic T_{reg} cells after inoculation of commensals, since neutralization of IL-2 in exGF mice significantly inhibited *Uhrf1* expression (**Fig. 3f**). In contrast, *Uhrf1* was not induced in splenic T_{reg} cells from exGF mice (**Supplementary Fig. 1e**). Consistent with our observations of exGF mice, there was substantial upregulation of *Uhrf1* in colonic T_{reg} cells during the population-expansion phase in infant SPF mice (**Supplementary Fig. 1c**).

To rigorously confirm the role of bacterial colonization in *Uhrf1* expression, we analyzed gnotobiotic mice colonized with a 17-strain mixture of Clostridia bacteria ('17-mix'), which efficiently induces the population expansion of T_{reg} cells in the colon[23]. Inoculation of GF mice with 17-mix significantly augmented IL-2 expression by T_{conv} cells (**Fig. 3g**), which led to upregulation of *Uhrf1* in T_{reg} cells, with a concomitant increase in their proliferation (**Fig. 3h,i**). We also confirmed the upregulation of *Uhrf1* in cultured T_{reg} cells stimulated with IL-2 (**Fig. 3j**), in which accumulation of the transcription factor STAT5 on the promoter region of *Uhrf1* was also evident (**Fig. 3k**). Together these results indicated that commensal bacteria upregulated *Uhrf1* in T_{reg} cells by eliciting IL-2 production from effector T cells (T_{eff} cells) in the colonic mucosa.

Uhrf1 is critical for colonic T_{reg} cell proliferation

To investigate the role of Uhrf1 in the homeostasis of colonic T_{reg} cells, we generated mice with T cell–specific deficiency in Uhrf1 (mice with *lox*P-flanked alleles (*Uhrf1*$^{fl/fl}$) deleted by Cre recombinase expressed from the Cd4 promoter (*Uhrf1*$^{fl/fl}$*Cd4*-Cre mice); **Supplementary Fig. 2a**) and crossed them with *Foxp3*^{hCD2} reporter mice (which have sequence encoding a reporter fusion of human CD52 and CD2 inserted into *Foxp3*), to easily detect T_{reg} cells[14], and thus generated *Uhrf1*$^{fl/fl}$*Cd4*-Cre*Foxp3*^{hCD2} progeny (called '*Uhrf1*$^{fl/fl}$*Cd4*-Cre' here). In young *Uhrf1*$^{fl/fl}$*Cd4*-Cre mice reared under SPF conditions, the overall composition of B lymphocytes and T lymphocytes was intact (**Supplementary Fig. 2b,c**). However, these mice had a considerable defect in the development of colonic T_{reg} cells (**Fig. 4a**) indicative of the importance of Uhrf1 in the homeostasis of T_{reg} cells in the colonic mucosa. We observed a slightly lower abundance of T_{reg} cells in the spleen and thymus of *Uhrf1*$^{fl/fl}$*Cd4*-Cre mice than in those of their *Uhrf1*$^{+/+}$*Cd4*-Cre (control) littermates (**Supplementary Fig. 2d**). We also confirmed the lower abundace of colonic T_{reg} cells in chimeras reconstituted with a mixture of bone marrow progenitor cells from Uhrf1-deficient and congenic wild-type mice. T_{reg} cells derived from the bone marrow of Uhrf1-deficient mice were nearly completely absent from the chimeras (**Supplementary Fig. 3a–c**). Thus, a T_{reg} cell–intrinsic defect was the cause of the lower abundance of these cells. Collectively, these data demonstrated that Uhrf1 was essential for the maintenance of colonic T_{reg} cells but not for the maintenance of extracolonic T_{reg} cells.

We further investigated whether Uhrf1 deficiency affected the differentiation or proliferation of T_{reg} cells by both *in vitro* and *in vivo* experiments. Uhrf1 deficiency did not influence the differentiation or stability of Foxp3 expression by T_{reg} cells in an *in vitro* culture system (**Fig. 4b** and data not shown). To rigorously confirm those results, we transferred naive $CD4^+$ T cells from Uhrf1-deficient or Uhrf1-sufficient $CD45.2^+$ mice into $CD45.1^+$ mice. The efficiency of T_{reg} cell differentiation *in vivo* was similar for Uhrf1-deficient and Uhrf1-sufficient naive T cells (**Supplementary Fig. 4a,b**). In contrast,

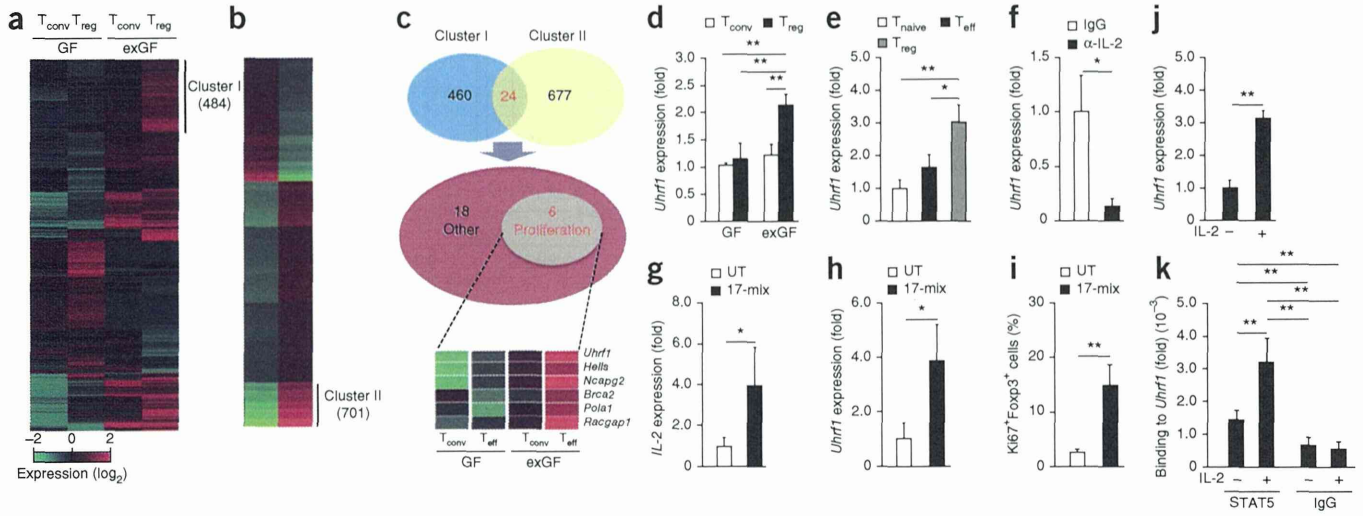

Figure 3 Colonization with commensal bacteria induces *Uhrf1* expression in colonic T_{reg} cells in IL-2-dependent manner. (**a**) Gene-expression profiles of T_{conv} cells ($CD3\varepsilon^+CD4^+CD25^-FR4^-$) and T_{reg} cells ($CD3\varepsilon^+CD4^+CD25^+FR4^+$) isolated from the cLP of GF and exGF mice. (**b**) Gene-expression profile of T_{reg} cells obtained from SPF mice and cultured *in vitro* and stimulated for 2 d with IL-2 in the presence of TGF-β. (**c**) Gene ontology–enrichment analysis of genes common to clusters I and II in **a**,**b**. (**d**) Quantitative PCR analysis of *Uhrf1* expression in T_{conv} cells and T_{reg} cells from the cLP of GF and exGF mice at 7 d after oral inoculation with feces from SPF C57BL/6 mice; results were normalized to those of the gene encoding β-actin (*Actb*) and are presented relative to those of T_{conv} cells from GF mice, set as 1. (**e**) *Uhrf1* expression in naive T cells (T_{naive}; $CD3\varepsilon^+CD4^+hCD2^-CD44^{lo}CD62L^{hi}$), T_{eff} cells ($CD3\varepsilon^+CD4^+hCD2^-CD44^{hi}CD62L^{lo}$) and T_{reg} cells $CD3\varepsilon^+CD4^+hCD2^+$) from SPF *Foxp3*^{hCD2} mice; results were normalized as in **d** and are presented relative to those of naive T cells, set as 1. (**f**) Quantitative PCR analysis of *Uhrf1* expression in cells from the cLP of mice inoculated orally with feces from SPF C57BL/6 mice and then, 3 d later, given intravenous injection of control IgG or neutralizing antibody to IL-2, followed by analysis 2 d later (at day 5); results were normalized as in **d** and are presented relative to those of cells from mice treated with IgG, set as 1. (**g**,**h**) Quantitative PCR analysis of the expression of *Il2* in T_{conv} cells (**g**) and *Uhrf1* in T_{reg} cells (**h**) from GF mice at day 3 (**g**) or day 6 (**h**) after inoculation with 17-mix; results were normalized to those of the gene encoding ribosomal protein L13A (*Rpl13a*) are presented relative to those of cells from untreated GF mice (UT), set as 1. (**i**) Frequency of $Foxp3^+Ki67^+$ cells in the cLP of GF mice at day 6 after inoculation with 17-mix, analyzed by flow cytometry (presented as in **g**,**h**). (**j**) Quantitative PCR analysis of *Uhrf1* expression in splenic $CD4^+CD25^+$ T cells cultured for 3 d with beads coated with mAb to CD3 and mAb to CD28 in the presence of IL-2 and TGF-β, allowed to 'rest' for 6 h and then stimulated 24 h with (+) or without (–) IL-2; results were normalized as in **g**,**h** and are presented relative to those of cells not stimulated with IL-2, set as 1. (**k**) ChIP–quantitative PCR analysis of the binding of STAT5 or IgG to the *Uhrf1* promoter region in splenic T cells cultured with beads as in **j**, allowed to 'rest' for 6 h and then stimulated for 1.5 h with or without IL-2; results are presented relative to total input. $^*P < 0.05$ and $^{**}P < 0.01$ (one-way ANOVA followed by Tukey's test (**d**,**e**,**k**), Mann-Whitney *U*-test (**f**,**g**,**i**) or Student's *t*-test (**h**,**j**)). Data are representative of one experiment (**a**–**c**,**g**–**k**;) or two experiments (**d**–**f**; error bars, s.e.m (**d**) or s.d. (**e**–**k**) of three mice per group).

Uhrf1 deficiency substantially adversely affected proliferation due to cell-cycle arrest at the G1-S transition (**Fig. 4c**,**d**). The same was true for Uhrf1-deficient T_{reg} cells in the cLP, as the frequency of $Ki67^+$ proliferating $Foxp3^+$ T_{reg} cells in the colon of *Uhrf1*$^{fl/fl}$*Cd4*-Cre mice was diminished (**Fig. 4e**,**f**). In contrast, the proliferation of T_{conv} cells was unaffected by Uhrf1 deficiency (**Fig. 4e**).

We further confirmed the role of Uhrf1 in T_{reg} cell homeostasis by another *in vivo* experiment. Although there was no difference between *Uhrf1*$^{fl/fl}$*Cd4*-Cre and *Uhrf1*$^{+/+}$*Cd4*-Cre mice in their proportion of T_{reg} cells under GF conditions (**Fig. 4g**), *Uhrf1*$^{fl/fl}$*Cd4*-Cre mice had defective population expansion of T_{reg} cells in response to colonization by chloroform-resistant bacteria, which consist of spore-forming bacteria mainly of the class Clostridia[1,24] (**Fig. 4h**). Thus, Uhrf1 was indispensable for the local population expansion of colonic T_{reg} cells.

Given that *Uhrf1* was an IL-2-responsive gene, we postulated the IL-2–Uhrf1 axis may serve a key role in the extensive proliferation of T_{reg} cells. To further investigate this possibility, we treated *Uhrf1*$^{fl/fl}$ *Cd4*-Cre and *Uhrf1*$^{+/+}$*Cd4*-Cre mice with exogenous IL-2 mixed with monoclonal antibody (mAb) to IL-2 (i.e., as a complex of IL-2 and mAb to IL-2). Consistent with a published report[25], this treatment potently induced a proliferative response in the systemic T_{reg} cell population specifically in *Uhrf1*$^{+/+}$*Cd4*-Cre mice; however, this response was substantially attenuated in the same population from *Uhrf1*$^{fl/fl}$*Cd4*-Cre mice (**Fig. 4i**). The complex of IL-2 and mAb to IL-2 also induced the proliferation of T_{conv} cells, albeit to a lesser extent than that of T_{reg} cells regardless of the presence of Uhrf1. These data provided evidence of the notable role of the IL-2–Uhrf1 axis in T_{reg} cell proliferation but the lesser role of this axis for T_{conv} cells.

Proliferation may confer functional maturity to T_{reg} cells[26], as shown by upregulation of the expression of molecules with a suppressive function in the proliferative compartment (**Supplementary Fig. 5a**). We hypothesized that diminished proliferative activity in the absence of Uhrf1 may affect the suppressive activity of T_{reg} cells. Indeed, ablation of Uhrf1 impaired the expression of functional molecules, including IL-10 and the immunomodulatory receptor CTLA-4 (CD152) (**Fig. 4j** and **Supplementary Fig. 5b**). Accordingly, Uhrf1-deficient T_{reg} cells exhibited attenuated immunosuppressive function and failed to prevent the development of experimental colitis (**Supplementary Fig. 6**). Given these observations, we concluded that Uhrf1 serves an essential role in the functional maturation of T_{reg} cells in the colonic mucosa, probably by regulating proliferation.

Uhrf1 epigenetically represses *Cdkn1a* expression

The Uhrf1-Dnmt1 complex has a critical role in the accurate maintenance of DNA methylation, which contributes to gene repression[16,17]. To define the targets of Uhrf1 that encode molecules involved in T_{reg} cell proliferation, we first profiled the subset of genes specifically derepressed only in T_{reg} cells (**Supplementary Fig. 7a**). Gene-function–enrichment analysis of the genes profiled identified at the top of the

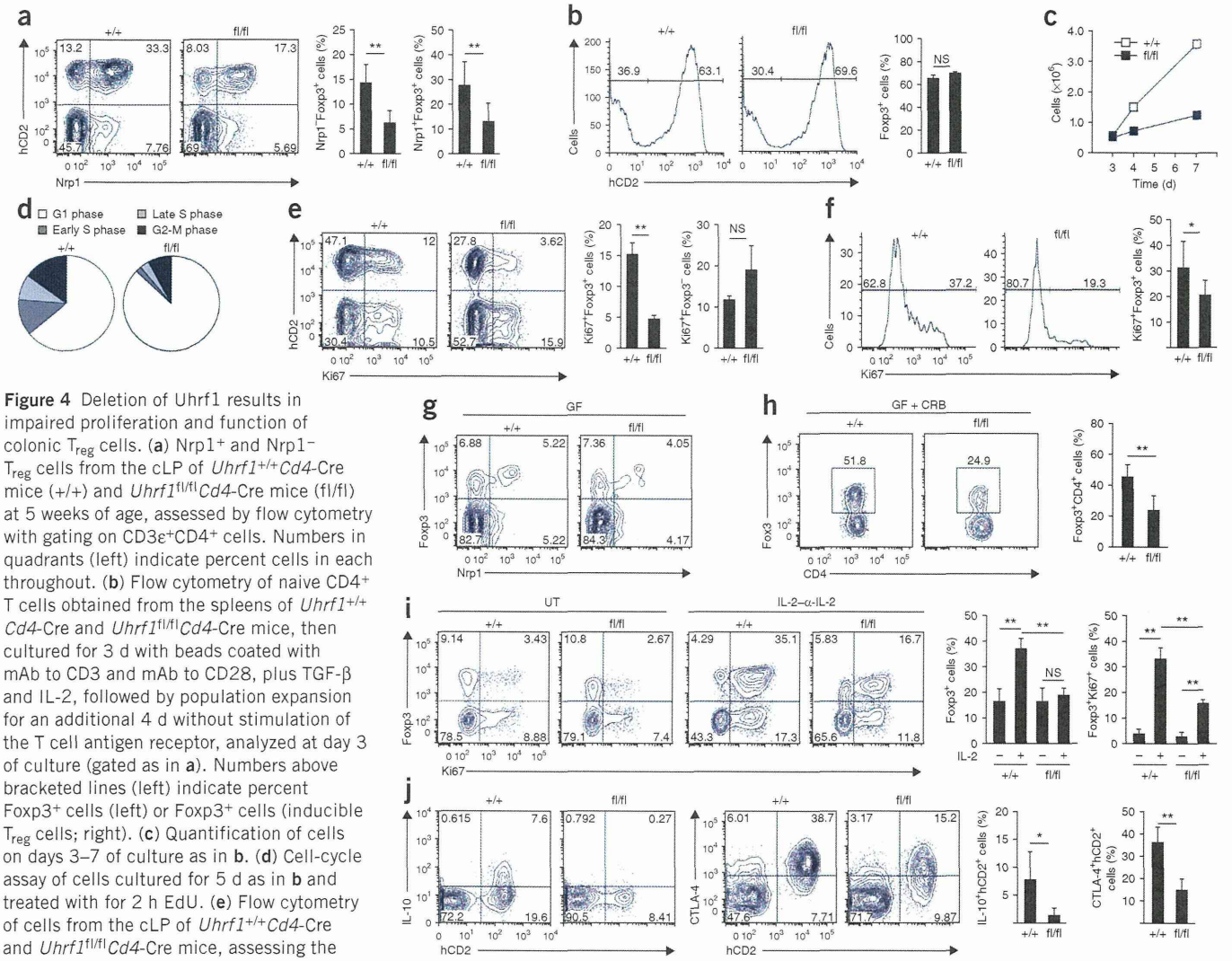

Figure 4 Deletion of Uhrf1 results in impaired proliferation and function of colonic T_{reg} cells. (**a**) Nrp1$^+$ and Nrp1$^-$ T_{reg} cells from the cLP of *Uhrf1*$^{+/+}$*Cd4*-Cre mice (+/+) and *Uhrf1*$^{fl/fl}$*Cd4*-Cre mice (fl/fl) at 5 weeks of age, assessed by flow cytometry with gating on CD3ε$^+$CD4$^+$ cells. Numbers in quadrants (left) indicate percent cells in each throughout. (**b**) Flow cytometry of naive CD4$^+$ T cells obtained from the spleens of *Uhrf1*$^{+/+}$*Cd4*-Cre and *Uhrf1*$^{fl/fl}$*Cd4*-Cre mice, then cultured for 3 d with beads coated with mAb to CD3 and mAb to CD28, plus TGF-β and IL-2, followed by population expansion for an additional 4 d without stimulation of the T cell antigen receptor, analyzed at day 3 of culture (gated as in **a**). Numbers above bracketed lines (left) indicate percent Foxp3$^+$ cells (left) or Foxp3$^+$ cells (inducible T_{reg} cells; right). (**c**) Quantification of cells on days 3–7 of culture as in **b**. (**d**) Cell-cycle assay of cells cultured for 5 d as in **b** and treated with for 2 h EdU. (**e**) Flow cytometry of cells from the cLP of *Uhrf1*$^{+/+}$*Cd4*-Cre and *Uhrf1*$^{fl/fl}$*Cd4*-Cre mice, assessing the frequency of Ki67$^+$ cells (gated as in **a**). (**f**) Flow cytometry of cells as in **e**, but with gating on CD3ε$^+$CD4$^+$Foxp3$^+$ cells. (**g**) Expression of Foxp3 and Nrp1 by CD4$^+$ T cells from the cLP of 8-week-old *Uhrf1*$^{+/+}$*Cd4*-Cre and *Uhrf1*$^{fl/fl}$*Cd4*-Cre mice reared under GF conditions, analyzed by flow cytometry (gated as in **a**). (**h**) Flow cytometry of CD4$^+$ T cells from the cLP of mice as in **g**, inoculated with chloroform-resistant bacteria (+ CRB) and analyzed 4 weeks later (gated as in **a**). Numbers adjacent to outline areas indicate percent Foxp3$^+$CD4$^+$ T cells. (**i**) Expression of Foxp3 and Ki67 by splenic CD4$^+$ T cells from *Uhrf1*$^{+/+}$*Cd4*-Cre and *Uhrf1*$^{fl/fl}$*Cd4*-Cre mice left untreated (UT) or treated with complexes of IL-2 and mAb to IL-2 (IL-2–α-IL-2), analyzed by flow cytometry (gated as in **a**). (**j**) Expression of IL-10 and CTLA-4 by Foxp3$^+$ cells from the cLP of *Uhrf1*$^{+/+}$*Cd4*-Cre and *Uhrf1*$^{fl/fl}$*Cd4*-Cre mice raised under SPF conditions, analyzed by flow cytometry (gated as in **a**). $^*P < 0.05$ and $^{**}P < 0.01$ (Student's *t* test (**a**,**e**,**f**,**h**,**j**), Mann-Whitney *U*-test (**b**) or one-way ANOVA followed by Tukey's test (**i**)). Data are representative of three independent experiments (error bars, s.d. of four to nine mice per group).

list (that is, among genes with the highest statistical significance) a group of genes encoding molecules in the category of 'cellular growth and proliferation' (**Supplementary Fig. 7b**,**c**). Furthermore, we used an integrated '-omics' approach with data sets obtained from the transcriptome and analysis of the 'methylome' (the pattern of methylated DNA in the genome) based on precipitation of methylated DNA followed by sequencing (MeDP-seq) (**Fig. 5a**) and identified *Cdkn1a* as a target of Uhrf1 (**Fig. 5b**). The product of *Cdkn1a*, p21, is a cell-cycle regulator that induces cell-cycle arrest at the G1-S transition[27]. We confirmed that there was substantially more *Cdkn1a* mRNA and p21 protein in *Uhrf1*$^{fl/fl}$*Cd4*-Cre T_{reg} cells than in *Uhrf1*$^{+/+}$*Cd4*-Cre T_{reg} cells (**Fig. 5c**,**d**). The derepression of *Cdkn1a* most probably resulted from hypomethylation of CpG islands in the distal promoter region of *Cdkn1a* in the absence of Uhrf1 (**Fig. 5e–g**), an outcome that was more prominent in T_{reg} cells than in T_{conv} cells (**Fig. 5f**). To further explore whether the derepression of *Cdkn1a* caused the cell-cycle arrest of *Uhrf1*$^{fl/fl}$*Cd4*-Cre T_{reg} cells, we induced *Uhrf1*$^{fl/fl}$*Cd4*-Cre cells *in vitro* to differentiate into T_{reg} cells, then treated those cells with small interfering RNA (siRNA) targeting *Cdkn1a* and analyzed their cell-cycle status. Knockdown of *Cdkn1a*, which diminished *Cdkn1a* expression by 45% (data not shown), at least partially rescued cells from the arrest at G1, as indicated by the greater proportion of cells in S phase than in G2-M phases (**Fig. 5h**). From these data, we concluded that Uhrf1-dependent repression of *Cdkn1a* was critical for the maintenance of T_{reg} cell proliferation.

Uhrf1-deficient mice spontaneously develop colitis

Intestinal T_{reg} cells orchestrate the immunoregulatory system that suppresses inappropriate immune responses to commensal bacteria[28].

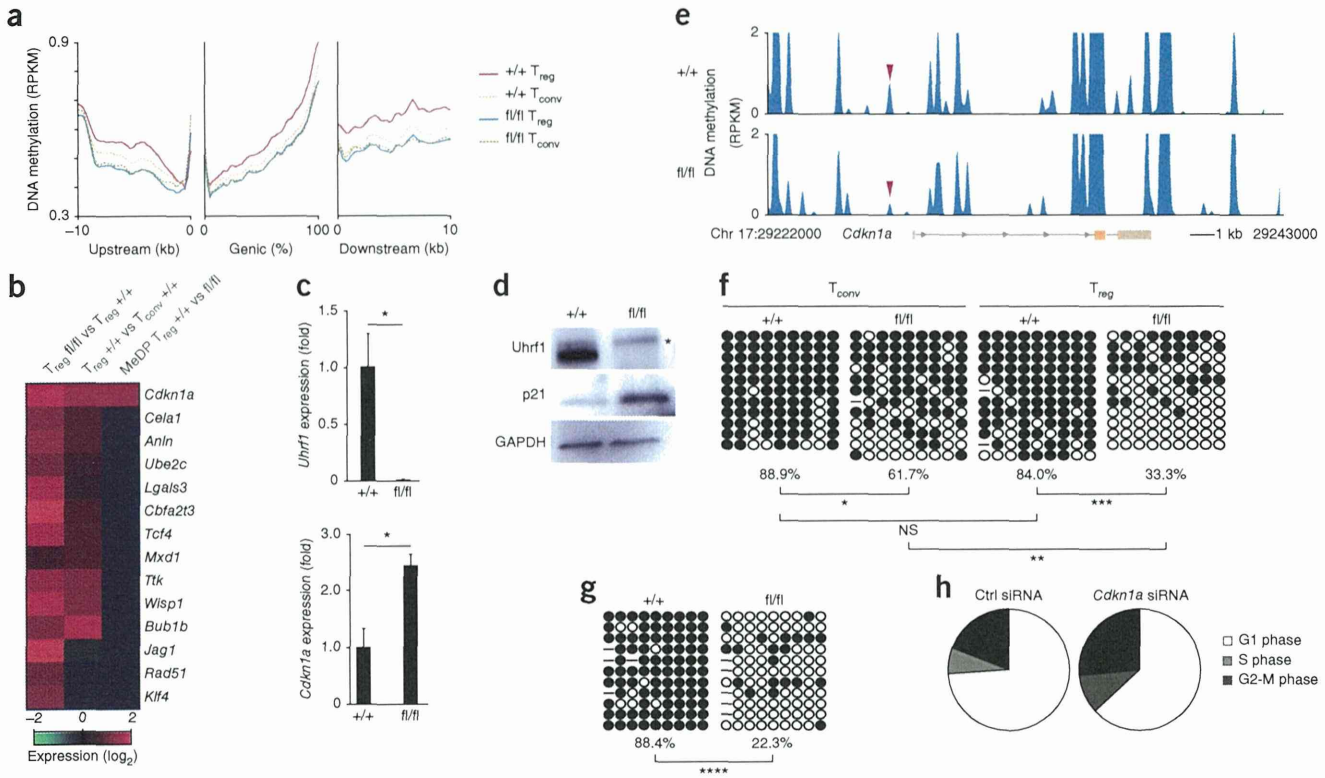

Figure 5 *Cdkn1a* is upregulated in Uhrf1-deficient T_{reg} cells because of hypomethylation of the *Cdkn1a* promoter region. (**a**) Genome-wide MeDP-seq analysis of DNA from *Uhrf1*$^{+/+}$*Cd4*-Cre and *Uhrf1*$^{fl/fl}$*Cd4*-Cre T_{conv} and T_{reg} cells, showing the average DNA methylation status (presented as 'reads' per kilobase of exon model per million mapped 'reads' (RPKM)) of upstream, genic and downstream regions. (**b**) Comparison of transcriptome analysis of *Uhrf1*$^{+/+}$*Cd4*-Cre and *Uhrf1*$^{fl/fl}$*Cd4*-Cre T_{reg} cells with the MeDP-seq analysis data to identify potential targets of Uhrf1 (right margin). (**c**) Quantitative PCR analysis of *Uhrf1* and *Cdkn1a* in *Uhrf1*$^{+/+}$*Cd4*-Cre and *Uhrf1*$^{fl/fl}$*Cd4*-Cre T_{reg} cells cultured *in vitro*; results are presented relative to those of *Uhrf1*$^{+/+}$*Cd4*-Cre cells, set as 1. $^{*}P < 0.01$ (Student's *t*-test). (**d**) Immunoblot analysis of Uhrf1 and p21 in *Uhrf1*$^{+/+}$*Cd4*-Cre and *Uhrf1*$^{fl/fl}$*Cd4*-Cre T_{reg} cells cultured *in vitro*; GAPDH (glyceraldehyde phosphate dehydrogenase) serves as a loading control. *, nonspecific signal. (**e**) MeDP-seq analysis of *Uhrf1*$^{+/+}$*Cd4*-Cre and *Uhrf1*$^{fl/fl}$*Cd4*-Cre CD3ε^{+}CD4^{+}hCD2^{+} cells *ex vivo*: red downward arrowheads, distal promoter region of *Cdkn1a* (exon structure below: orange, coding sequences; tan, UTR; arrows, direction of transcription). (**f**,**g**) Bisulfite-sequencing analysis of the methylation of CpG islands on the distal promoter region of *Cdkn1a* in *Uhrf1*$^{+/+}$*Cd4*-Cre and *Uhrf1*$^{fl/fl}$*Cd4*-Cre T_{conv} and T_{reg} cells *ex vivo* (**f**) and T_{reg} cells cultured *in vitro* (**g**): filled circles, methylated; open circles, demethylated; –, undetermined (due to noise signals); below, methylated CpG/total CpG. $^{*}P = 5.94 \times 10^{-5}$, $^{**}P = 4.34 \times 10^{-13}$, $^{***}P = 7.18 \times 10^{-14}$ and $^{****}P = 3.12 \times 10^{-21}$ (hypergeometric distribution). (**h**) Cell-cycle assay of *Uhrf1*$^{+/+}$*Cd4*-Cre naive CD4^{+} T cells differentiated into Foxp3^{+} cells, then treated for 24 h with fluorescence-labeled *Cdkn1a*-specific siRNA (*Cdkn1a* siRNA) or nontargeting (control) siRNA (Ctrl siRNA). Data are representative of two (**a**,**b**,**e**–**g**) or three (**c**,**d**,**h**) independent experiments.

Given that the absence of Uhrf1 led to a considerable defect in the accumulation of colonic T_{reg} cells, we reasoned that Uhrf1 might be fundamental to the maintenance of intestinal immunological homeostasis. In support of that proposal, *Uhrf1*$^{fl/fl}$*Cd4*-Cre mice spontaneously developed colitis characterized by thickening of the colonic wall, epithelial hyperplasia, loss of goblet cells and massive cellular infiltrates into the colonic mucosa and submucosa before 10 weeks of age (**Fig. 6a–d** and **Supplementary Fig. 8a**). Nearly all of the *Uhrf1*$^{fl/fl}$*Cd4*-Cre mice eventually succumbed to death within 6 months due to the exacerbated colitis (data not shown). In contrast, there were no inflammatory symptoms in the other peripheral tissues examined, including liver, kidney, lung, skin, pancreas, stomach, salivary gland and small intestine (**Supplementary Fig. 9**), consistent with the observation that the Uhrf1-regulated population expansion of T_{reg} cells occurred principally in the local colonic mucosa (**Figs. 1–4** and **Supplementary Figs. 1** and **2**). Commensal bacteria were the causative agent of this chronic inflammatory response, because *Uhrf1*$^{fl/fl}$*Cd4*-Cre mice raised under GF conditions did not display any inflammation (**Supplementary Fig. 8b–d**).

We subsequently examined the immunological phenotype of the spontaneous colitis. The expression of genes encoding proinflammatory cytokines was upregulated considerably in *Uhrf1*$^{fl/fl}$*Cd4*-Cre mice relative to their expression in *Uhrf1*$^{+/+}$*Cd4*-Cre mice (**Fig. 6e**). In keeping with that, the frequency of T_{eff} cells expressing the proinflammatory cytokines interferon-γ, IL-17A and tumor-necrosis factor in the cLP was much greater in *Uhrf1*$^{fl/fl}$*Cd4*-Cre mice than in *Uhrf1*$^{+/+}$*Cd4*-Cre mice (**Fig. 6f,g**). Conversely, IL-10-expressing T_{reg} cells were nearly absent from colitic *Uhrf1*$^{fl/fl}$*Cd4*-Cre mice (**Fig. 6f,g**). This was also the case even in younger mice before the development of frank colitis (**Fig. 4j**). These results suggested that activation of responses of the T_H1 and T_H17 subsets of helper T cells due to compromised T_{reg} cell function mediated the development of colitis in *Uhrf1*$^{fl/fl}$*Cd4*-Cre mice.

To investigate the possibility that excessive activation of T_{eff} cells due to the loss of Uhrf1 might cause the development of colitis, we assessed the *in vivo* function of T_{eff} cells independently of the effect of T_{reg} cell dysfunction through the use of a mixed–bone marrow chimera system. We transferred CD45.1^{+} wild-type and Uhrf1-deficient

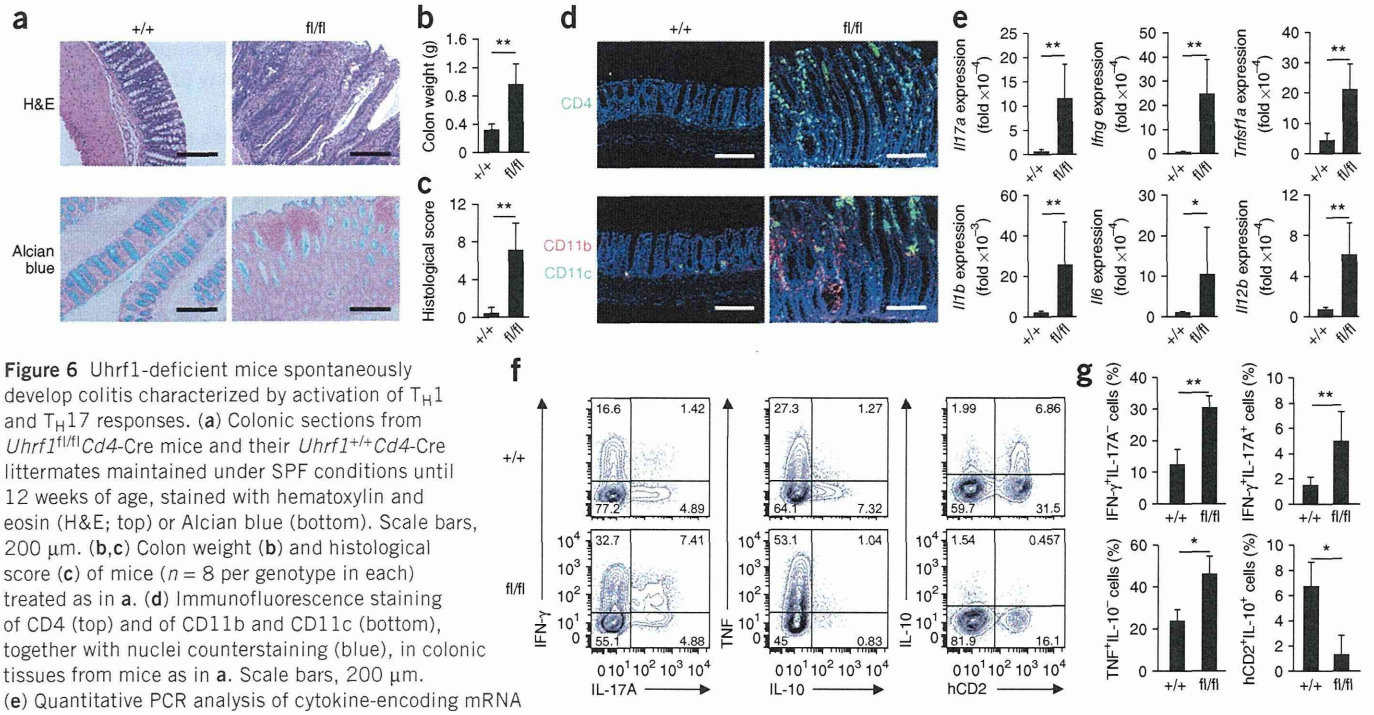

Figure 6 Uhrf1-deficient mice spontaneously develop colitis characterized by activation of T_H1 and T_H17 responses. (**a**) Colonic sections from *Uhrf1*$^{fl/fl}$*Cd4*-Cre mice and their *Uhrf1*$^{+/+}$*Cd4*-Cre littermates maintained under SPF conditions until 12 weeks of age, stained with hematoxylin and eosin (H&E; top) or Alcian blue (bottom). Scale bars, 200 μm. (**b**,**c**) Colon weight (**b**) and histological score (**c**) of mice ($n = 8$ per genotype in each) treated as in **a**. (**d**) Immunofluorescence staining of CD4 (top) and of CD11b and CD11c (bottom), together with nuclei counterstaining (blue), in colonic tissues from mice as in **a**. Scale bars, 200 μm. (**e**) Quantitative PCR analysis of cytokine-encoding mRNA in colonic tissue from mice as in **a** ($n = 11$); results are presented relative to *Actb* expression. (**f**,**g**) Cytokine expression in cLP-infiltrating CD4$^+$ T cells from mice as in **a**, analyzed by flow cytometry (**f**) and summarized (**g**). $^*P < 0.05$ and $^{**}P < 0.01$ (Mann-Whitney *U* test (**b**,**c**,**e**) or Student's *t*-test (**g**)). Data are representative of three independent experiments (error bars (**b**,**c**,**e**,**g**), s.d.).

bone marrow cells together into irradiated recipient mice with congenital deficiency in mature B cells and T cells (deficient in recombination-activating gene 1). We confirmed that these chimeras did not show any signs of inflammation in the colon (data not shown). Under these non-inflammatory conditions, the frequency of T_{eff} cells expressing interferon-γ and IL-17A in the cLP was similar for Uhrf1-deficient and Uhrf1-sufficient populations (**Supplementary Fig. 3d**). In addition, Uhrf1 deficiency did not influence the *in vitro* differentiation or function of the T_{eff} cells (**Supplementary Fig. 10a**,**b**). Examination of methylated DNA by MeDP-seq analysis also confirmed that the methylation status of genes encoding proinflammatory cytokines, as well as those encoding key transcription factors for T_H1 or T_H17 differentiation, was normal in the absence of Uhrf1 (**Supplementary Fig. 10c–f**). These results excluded the possibility that deficiency of Uhrf1 influenced the function of colonic T_{eff} cells.

We finally investigated whether the defect in T_{reg} cell proliferation was responsible for the development of colitis. To address this issue, we gave young (4- to 5-week-old) *Uhrf1*$^{fl/fl}$*Cd4*-Cre mice wild-type T_{reg} cells (CD3$^+$CD4$^+$CD45.1$^+$hCD2$^+$ cells) from congenic *Foxp3*^{hCD2} reporter mice. Adoptive transfer of the wild-type T_{reg} cells prevented the development of colitis (**Fig. 7a**), concomitant with suppression of the T_{eff} cell response (**Fig. 7b**). Collectively, these data illustrated that the aberrant activation of T_{eff} cells caused by Uhrf1 deficiency resulted from the breakdown of the colonic immunoregulatory system. From this model, we concluded that the proliferative response of T_{reg} cells mediated by Uhrf1 was a prerequisite for their functional maturation in colonic mucosa.

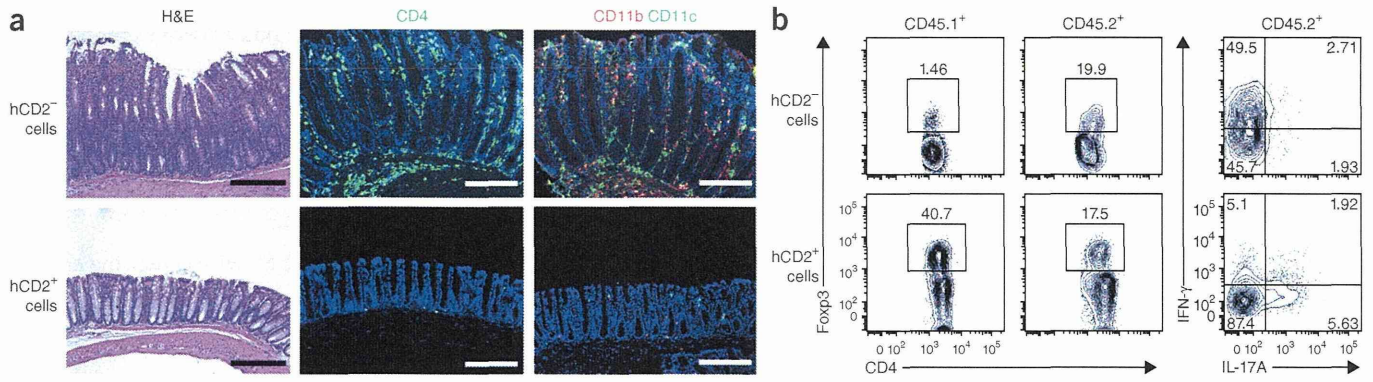

Figure 7 A defect in the proliferation of colonic T_{reg} cells is responsible for the development of spontaneous colitis in *Uhrf1*$^{fl/fl}$*Cd4*-Cre mice. (**a**) Histology and immunofluorescence staining of colonic tissues from *Uhrf1*$^{fl/fl}$*Cd4*-Cre mice (6 weeks of age) at 6 weeks after transfer of hCD2$^+$ or hCD2$^-$ cells from CD45.1$^+$ congenic *Foxp3*^{hCD2} mice. Scale bars, 200 μm. (**b**) Flow cytometry of CD4$^+$ T cells from cLP of the mice in **a**. Numbers adjacent to outlined areas (left and middle) indicate percent Foxp3$^+$CD4$^+$ cells. Data are representative of two independent experiments (with a total of four mice per group) with similar results.

DISCUSSION

Multiple lines of evidence support the concept that dysregulation of the intestinal immune response to commensal microbes is a predisposing factor for inflammatory bowel disease[5,29–31]. Such chronic inflammatory responses compromise the homeostasis of the intestinal ecosystem and often result in dysbiosis[32,33]. Therefore, commensal microbes may have undergone adaptation to curtail host immune responses over the course of coevolution[1–3]. We have now demonstrated that bacterial colonization induced an early IL-2 response in the colonic mucosa that in turn led to the accumulation of T_{reg} cells, at least in part through vigorous proliferation, that overwhelmed the activation of T_{eff} cells. The local proliferative activity of colonic T_{reg} cells was maximal before weaning and gradually decreased with age. This suggested that vigorous proliferation of colonic T_{reg} cells was induced early after birth in parallel with the establishment of the commensal microflora. This model was congruent with the observation that the expression of *Uhrf1* was much higher in colonic T_{reg} cells from 2-week-old infant mice than in those from adult mice. Similarly, *Uhrf1* expression by colonic T_{reg} cells was upregulated after the inoculation of GF mice with intestinal microflora. In contrast, *Uhrf1* expression by splenic T_{reg} cells of the same mice remained unchanged before and after the inoculation, consistent with the minimal proliferative response in the spleen. Thus, the expression of *Uhrf1* was positively correlated with the proliferative activity of T_{reg} cells, and Uhrf1 deficiency had a substantial effect on the local population expansion of T_{reg} cells in response to bacterial colonization. The data as a whole supported our conclusion that local proliferation of T_{reg} cells was the main downstream consequence of Uhrf1 expression. Notably, the ablation of Uhrf1 had a substantial effect on the suppressive function of T_{reg} cells. We propose that this defect was due to the compromised proliferative response of Uhrf1-deficient T_{reg} cells, because proliferating T_{reg} cells had higher expression of functional molecules than did cells in the nonproliferative compartment. Therefore, colonic tissue acts as a privileged site in conferring functional maturity on T_{reg} cells. Given that Uhrf1-deficient mice spontaneously developed colitis, this immunoregulatory mechanism ensured by Uhrf1-dependent proliferation of T_{reg} cells was essential for the establishment of a symbiotic host-microbe relationship without inflammation.

Our data identified Uhrf1 as an IL-2-responsive molecule. In the intestine, both T cells and dendritic cells can produce IL-2 (refs. 34,35). We also confirmed that IL-2 was produced by both T cell populations and non-T cell populations, among which $CD4^+$ T cells mainly contributed to IL-2 production after colonization by commensals (data not shown). We found that colonization with the '17-mix' strains of Clostridia from human feces[23] drove T_{conv} cells to produce IL-2, which in turn upregulated *Uhrf1* in T_{reg} cells; this resulted in their active proliferation. In our *ex vivo* experiments, T_{conv} cells from mice colonized with 17-mix produced IL-2 only in the presence of autoclaved 17-mix (data not shown), which indicated that some of the T_{conv} cells in the mice colonized with 17-mix produced IL-2 in an antigen-specific manner. These observations raise the possibility that stimulation of T cells through the T cell antigen receptor with bacterial antigens may initiate activation of the IL-2–Uhrf1 pathway.

Like Uhrf1-deficient mice, mice lacking either IL-2 or one of its receptors (IL-2Rα or IL-2Rβ) spontaneously develop chronic colitis due to an excessive response to commensal bacteria[36,37]. Moreover, these mice develop lethal lymphoid hyperplasia and autoimmune disorders characterized by hemolytic anemia[38,39]. We did not observe such systemic autoimmune disorders in Uhrf1-deficient mice. Therefore, among the many biological functions of IL-2, the role of the IL-2–Uhrf1 pathway is itself confined to the maintenance of gut immunological homeostasis. Given that genetic polymorphisms in *IL2* and *IL2RA* are closely associated with the development of human inflammatory bowel disease[40], our findings may provide molecular insight into the pathogenesis of this disease.

We identified *Cdkn1a* (which encodes p21) as a target of Uhrf1 and showed the importance of the Uhrf1-p21 axis in the proliferation of T_{reg} cells. p21 has a vital role in controlling the proliferation, differentiation and tumorigenesis of many cell types[41]. The mechanisms for the regulation of *Cdkn1a* transcription are not yet fully elucidated, although it seems to be regulated via multiple pathways that may be different in various cell types. A possible link between Uhrf1 and p21 has been reported in embryonic stem cells and HeLa human cervical cancer cells[42]. The authors of that study[42] speculate that Uhrf1 recruits the histone lysine methyltransferase G9a to the *Cdkn1a* promoter to achieve accumulation of the repressive histone modification H3K9me2. *Cdkn1a* has a proximal promoter and a distal promoter in which CpG islands and a CpG cluster, respectively, are present. In intestinal epithelial cells, the proximal promoter is almost completely unmethylated; however, the distal promoter is partially methylated, which is negatively correlated with *Cdkn1a* expression[43]. In agreement with that observation, deficiency in Uhrf1 led to aberrant expression of *Cdkn1a* due to hypomethylation of its distal promoter region in T_{reg} cells. It is well documented that signaling via transforming growth factor-β (TGF-β) transactivates *Cdkn1a* expression as a canonical pathway[44,45]. Given that TGF-β, which is abundant in the intestinal tissue, is essential for the induction and maintenance of T_{reg} cells, it is conceivable that intestinal T_{reg} cells may be under continuous pressure to upregulate *Cdkn1a*. In this context, Uhrf1-dependent methylation of CpG sites may function to prevent the unwanted *Cdkn1a* expression that leads to a disadvantage in the progression of T_{reg} cells through the cell cycle.

Taking all of the observations noted above into account, we propose a model for establishment of gut immunological homeostasis based on reciprocal interaction between T_{reg} cells and T_{eff} cells. First, colonizing bacteria should be initially recognized by antigen-presenting cells such as dendritic cells. Second, the antigen-loaded antigen-presenting cells elicit an early IL-2 response by stimulating T_{eff} cells through antigen presentation. Third, the early IL-2 reponse provides a cue for T_{reg} cells to proliferate and simultaneously upregulate *Uhrf1* expression. Fourth, Uhrf1 represses the cell cycle–dependent kinase inhibitor p21 via methylation of *Cdkn1a* (which encodes p21) to safeguard the continuing proliferation of T_{reg} cells. Fifth, the actively proliferating T_{reg} cells become functionally mature and in turn prevent excessive immune responses to the colonizing microbiota. In conclusion, our study has provided a new mechanistic link between proliferation-dependent maturation of T_{reg} cells and containment of the inflammatory response to commensal microbiota.

METHODS

Methods and any associated references are available in the online version of the paper.

Accession codes. GEO: microarray and MeDP-Sequencing analysis data, GSE56544.

Note: Any Supplementary Information and Source Data files are available in the online version of the paper.

ACKNOWLEDGMENTS

We thank P.D. Burrows for critical reading and editing of the manuscript; T. Mukai, M. Yoshida, P. Carnincci, Y. Shinkai and H. Kiyono for comments and suggestions; and S. Fukuda and Y. Koseki for technical support. Supported by the Japan Society for the Promotion of Science (24117723 and 25293114 to K. Ha., 24890293 to

Y.F. and 252667 to Y.O.), the Japan Science and Technology Agency (PRESTO to K. Ha.), the RIKEN RCAI-IMS Young Chief Investigator program (K. Ha.), the RIKEN RCAI-IMS Open Laboratory for Allergy Research Project (T.D.), the Kato Memorial Bioscience Foundation (Y.F.), The Uehara Memorial Foundation (K. Ha.), the Mochida Memorial Foundation for Medical and Pharmaceutical Research (K. Ha.), the Toray Science Foundation (K. Ha.) and the National Center for Global Health and Medicine (21-110 and 22-205 to T.D.).

AUTHOR CONTRIBUTIONS

Y.O. and Y.F. did a large part of the experiments together with D.T., K.A., Y.F., M.T., T.I., T.O., Y.I.K. and K. Ha.; Y.O., Y.F., T.A.E. and J.S. analyzed the data; M.N., S.T. and S.H. provided materials; S.O. prepared GF mice; T.D., H.M., O.O., K. Ho., H.O. and H.K. provided experimental protocols and intellectual input into the study; T.D. and H.O. edited the manuscript; K. Ha. and H.K. conceived of the study; and K. Ha. designed the experiments, analyzed the data and wrote the manuscript (together with Y.O. and Y.F.).

COMPETING FINANCIAL INTERESTS

The authors declare no competing financial interests.

1. Atarashi, K. *et al.* Induction of colonic regulatory T cells by indigenous Clostridium species. *Science* **331**, 337–341 (2011).
2. Round, J.L. & Mazmanian, S.K. Inducible Foxp3+ regulatory T-cell development by a commensal bacterium of the intestinal microbiota. *Proc. Natl. Acad. Sci. USA* **107**, 12204–12209 (2010).
3. Geuking, M.B. *et al.* Intestinal bacterial colonization induces mutualistic regulatory T cell responses. *Immunity* **34**, 794–806 (2011).
4. Round, J.L. *et al.* The Toll-like receptor 2 pathway establishes colonization by a commensal of the human microbiota. *Science* **332**, 974–977 (2011).
5. Round, J.L. & Mazmanian, S.K. The gut microbiota shapes intestinal immune responses during health and disease. *Nat. Rev. Immunol.* **9**, 313–323 (2009).
6. Park, S.-G. *et al.* T regulatory cells maintain intestinal homeostasis by suppressing γδ T cells. *Immunity* **33**, 791–803 (2010).
7. Furusawa, Y. *et al.* Commensal microbe-derived butyrate induces the differentiation of colonic regulatory T cells. *Nature* doi:10.1038/nature12721 (2013).
8. Smith, P.M. *et al.* The microbial metabolites, short-chain fatty acids, regulate colonic Treg cell homeostasis. *Science* **341**, 569–573 (2013).
9. Arpaia, N. *et al.* Metabolites produced by commensal bacteria promote peripheral regulatory T-cell generation. *Nature* **504**, 451–455 (2013).
10. Singh, N. *et al.* Activation of gpr109a, receptor for niacin and the commensal metabolite butyrate, suppresses colonic inflammation and carcinogenesis. *Immunity* **40**, 128–139 (2014).
11. Kim, S.V. *et al.* GPR15-mediated homing controls immune homeostasis in the large intestine mucosa. *Science* **340**, 1456–1459 (2013).
12. Berger, S.L., Kouzarides, T., Shiekhattar, R. & Shilatifard, A. An operational definition of epigenetics. *Genes Dev.* **23**, 781–783 (2009).
13. Zheng, Y. *et al.* Role of conserved non-coding DNA elements in the *Foxp3* gene in regulatory T-cell fate. *Nature* **463**, 808–812 (2010).
14. Miyao, T. *et al.* Plasticity of Foxp3+ T cells reflects promiscuous Foxp3 expression in conventional T cells but not reprogramming of regulatory T cells. *Immunity* **36**, 262–275 (2012).
15. Ohkura, N. *et al.* T cell receptor stimulation-induced epigenetic changes and Foxp3 expression are independent and complementary events required for Treg cell development. *Immunity* **37**, 785–799 (2012).
16. Bostick, M. *et al.* UHRF1 plays a role in maintaining DNA methylation in mammalian cells. *Science* **317**, 1760–1764 (2007).
17. Sharif, J. *et al.* The SRA protein Np95 mediates epigenetic inheritance by recruiting Dnmt1 to methylated DNA. *Nature* **450**, 908–912 (2007).
18. Unoki, M., Nishidate, T. & Nakamura, Y. ICBP90, an E2F-1 target, recruits HDAC1 and binds to methyl-CpG through its SRA domain. *Oncogene* **23**, 7601–7610 (2004).
19. Nishiyama, A. *et al.* Uhrf1-dependent H3K23 ubiquitylation couples maintenance DNA methylation and replication. *Nature* **502**, 249–253 (2013).
20. Yadav, M. *et al.* Neuropilin-1 distinguishes natural and inducible regulatory T cells among regulatory T cell subsets *in vivo*. *J. Exp. Med.* **209**, 1713–1722 (2012).
21. Weiss, J.M. *et al.* Neuropilin 1 is expressed on thymus-derived natural regulatory T cells, but not mucosa-generated induced Foxp3+ T reg cells. *J. Exp. Med.* **209**, 1723–1742 (2012).
22. Fontenot, J.D., Rasmussen, J.P., Gavin, M.A. & Rudensky, A.Y. A function for interleukin 2 in Foxp3-expressing regulatory T cells. *Nat. Immunol.* **6**, 1142–1151 (2005).
23. Atarashi, K. *et al.* Treg induction by a rationally selected mixture of *Clostridia* strains from the human microbiota. *Nature* **500**, 232–236 (2013).
24. Itoh, K. & Mitsuoka, T. Characterization of clostridia isolated from faeces of limited flora mice and their effect on caecal size when associated with germ-free mice. *Lab. Anim.* **19**, 111–118 (1985).
25. Webster, K.E. *et al. In vivo* expansion of T reg cells with IL-2-mAb complexes: induction of resistance to EAE and long-term acceptance of islet allografts without immunosuppression. *J. Exp. Med.* **206**, 751–760 (2009).
26. Barthlott, T. *et al.* CD25+CD4+ T cells compete with naive CD4+ T cells for IL-2 and exploit it for the induction of IL-10 production. *Int. Immunol.* **17**, 279–288 (2005).
27. Deng, C., Zhang, P., Harper, J.W., Elledge, S.J. & Leder, P. Mice lacking p21CIP1/WAF1 undergo normal development, but are defective in G1 checkpoint control. *Cell* **82**, 675–684 (1995).
28. Powrie, F., Leach, M.W., Mauze, S., Caddle, L.B. & Coffman, R.L. Phenotypically distinct subsets of CD4+ T cells induce or protect from chronic intestinal inflammation in C. B-17 scid mice. *Int. Immunol.* **5**, 1461–1471 (1993).
29. Sellon, R.K. *et al.* Resident enteric bacteria are necessary for development of spontaneous colitis and immune system activation in interleukin-10-deficient mice. *Infect. Immun.* **66**, 5224–5231 (1998).
30. Manichanh, C., Borruel, N., Casellas, F. & Guarner, F. The gut microbiota in IBD. *Nat Rev Gastroenterol Hepatol* **9**, 599–608 (2012).
31. Sartor, R.B. Microbial influences in inflammatory bowel diseases. *Gastroenterology* **134**, 577–594 (2008).
32. Clemente, J.C., Ursell, L.K., Parfrey, L.W. & Knight, R. The impact of the gut microbiota on human health: an integrative view. *Cell* **148**, 1258–1270 (2012).
33. Winter, S.E. *et al.* Host-derived nitrate boosts growth of *E. coli* in the inflamed gut. *Science* **339**, 708–711 (2013).
34. Granucci, F. *et al.* Inducible IL-2 production by dendritic cells revealed by global gene expression analysis. *Nat. Immunol.* **2**, 882–888 (2001).
35. Han, D. *et al.* Dendritic cell expression of the signaling molecule TRAF6 is critical for gut microbiota-dependent immune tolerance. *Immunity* **38**, 1211–1222 (2013).
36. Sadlack, B. *et al.* Ulcerative colitis-like disease in mice with a disrupted interleukin-2 gene. *Cell* **75**, 253–261 (1993).
37. Ehrhardt, R.O., Lúdvíksson, B.R., Gray, B., Neurath, M. & Strober, W. Induction and prevention of colonic inflammation in IL-2-deficient mice. *J. Immunol.* **158**, 566–573 (1997).
38. Willerford, D.M. *et al.* Interleukin-2 receptor alpha chain regulates the size and content of the peripheral lymphoid compartment. *Immunity* **3**, 521–530 (1995).
39. Suzuki, H. *et al.* Deregulated T cell activation and autoimmunity in mice lacking interleukin-2 receptor β. *Science* **268**, 1472–1476 (1995).
40. Jostins, L. *et al.* Host-microbe interactions have shaped the genetic architecture of inflammatory bowel disease. *Nature* **491**, 119–124 (2012).
41. Sherr, C.J. & Roberts, J.M. CDK inhibitors: positive and negative regulators of G1-phase progression. *Genes Dev.* **13**, 1501–1512 (1999).
42. Kim, J.K., Estève, P.-O., Jacobsen, S.E. & Pradhan, S. UHRF1 binds G9a and participates in p21 transcriptional regulation in mammalian cells. *Nucleic Acids Res.* **37**, 493–505 (2009).
43. Yang, W., Bancroft, L. & Augenlicht, L.H. Methylation in the p21WAF1/cip1 promoter of Apc+/–, p21+/– mice and lack of response to sulindac. *Oncogene* **24**, 2104–2109 (2005).
44. Pardali, K. *et al.* Role of Smad proteins and transcription factor Sp1 in p21(Waf1/Cip1) regulation by transforming growth factor-β. *J. Biol. Chem.* **275**, 29244–29256 (2000).
45. Cordenonsi, M. *et al.* Links between tumor suppressors: p53 is required for TGF-β gene responses by cooperating with Smads. *Cell* **113**, 301–314 (2003).

ONLINE METHODS

Animal experiments. *Uhrf1*$^{fl/fl}$ mice (generated as in **Supplementary Fig. 2**) were backcrossed onto a C57BL/6 background. For the generation of mice with T cell-specific Uhrf1 deficiency, *Uhrf1*$^{fl/fl}$ mice were crossed with *Cd4*-Cre mice (The Jackson Laboratory) and then *Foxp3*^{hCD2} mice[14]. *Uhrf1*$^{fl/fl}$*Cd4*-Cre*Foxp3*^{hCD2} mice were housed under SPF conditions unless otherwise specified. IQI mice (CLEA Japan) were maintained in GF conditions in vinyl isolators in the animal facilities of the RIKEN Center for Integrative Medical Sciences and Graduate School of Medical Life Science, Yokohama City University. Feces from SPF C57BL/6 mice were suspended in PBS or were treated with 3% (vol/vol) chloroform in PBS to generate chloroform-resistant bacteria, and GF IQI and *Uhrf1*$^{fl/fl}$*Cd4*-Cre *Foxp3*^{hCD2} mice were inoculated with aliquots of those suspensions by intragastric intubation[1]. Mice treated with chloroform-resistant bacteria were maintained in the gnotobiotic vinyl isolator for 3–4 weeks. Gnotobiotic mice associated with the 17-strain mixture of Clostridia (17-mix) were generated as described[23].

For inhibition of the homing of extraintestinal T_{reg} cells to the gut[11], exGF mice were treated with a mixture (100 μg each per mouse) of mAb to integrin α4 (PS/2; Millipore) plus mAb to integrin β_7 (FIB504; Biolegend) or with control IgG (400533; Biolegend) on day 3 after bacterial colonization. The exGF mice were then subjected to an *in vivo* EdU-incorporation assay as described below.

Systemic population expansion of T_{reg} cells was induced as described[25]. SPF *Uhrf1*$^{fl/fl}$*Cd4*-Cre*Foxp3*^{hCD2} mice and their *Uhrf1*$^{+/+}$*Cd4*-Cre*Foxp3*^{hCD2} littermates were given intraperitoneal injection of complexes of IL-2 and mAb to IL-2 (JES6-1A12; R&D Systems) three times on days 0, 1 and 2, and proliferation of splenic T_{reg} cells was analyzed on day 5.

Protocols approved by Animal Studies Committees of RIKEN Yokohama Institute, The Institute of Medical Science, The University of Tokyo and Graduate School of Medical Life Science, Yokohama City University, were used for all animal experiments.

Preparation of lymphocytes. Lymphocytes from the cLP were prepared as described[46]. Colonic tissues were treated at 37 °C for 20 min with Hanks' balanced-salt solution (Wako Pure Chemical Industries) containing 1 mM dithiothreitol and 20 mM EDTA for removal of epithelial cells. The tissues were then minced and were dissociated for 30 min at 37 °C with collagenase solution containing 0.5 mg/ml collagenase (Wako Pure Chemical Industries) and 0.5 mg/ml DNase I (Roche Diagnostics), 2% FCS, 100 U/ml penicillin, 100 μg/ml streptomycin and 12.5 mM HEPES, pH 7.2, in RPMI-1640 medium (Sigma-Aldrich) to obtain single-cell suspensions. After filtration, the single-cell suspensions were washed with 2% FCS in RPMI-1640 medium and were subjected to Percoll gradient separation. The spleen and mesenteric lymph nodes were mechanically disrupted into single-cell suspensions.

For quantitative PCR analysis, colonic mononuclear cells was subjected to cell sorting using FACSAriaII to isolate CD3ε$^+$CD4$^+$CD25$^+$FR4$^+$ or CD3ε$^+$CD4$^+$hCD2$^+$ T_{reg} cells, in IQI or Foxp3^{hCD2} reporter mice, respectively. Our preliminary experiments demonstrated that the CD3ε$^+$CD4$^+$CD25$^+$FR4$^+$ population almost exclusively consists of Foxp3$^+$ cells, consistent with a previous report[47].

Flow cytometry. The following mAbs were conjugated to biotin, fluorescein isothiocyanate, Alexa Fluor 488, phycoerythrin, peridinin chlorophyll protein–cyanine 5.5, phycoerythrin-indotricarbocyanine, allophycocyanin, Alexa Fluor 647, Alexa Fluor 700, allophycocyanin-Hilite7, eFluor 450, Pacific blue, Brilliant violet 421 or V500: anti–human CD2 (RPA-2.10), mAb to mouse CD25 (PC61), mAb to mouse CD44 (IM7), mAb to mouse CD45R/B220 (RA3-6B2), mAb to mouse CD62L (MEL-14), mAb to mouse Gr1 (RB6-8C5), mAb to mouse IL-2 (JES6-5H4), mAb to mouse interferon-γ (XMG1.2), mAb to mouse tumor-necrosis factor (MP6-XT22) and mAb to mouse Ter119 (TER-119; all from Biolegend); mAb to mouse CD3ε (145-2C11), mAb to mouse folate receptor 4 (eBio12A5), mAb to mouse Foxp3 (FJK-16s), mAb to mouse CTLA-4 (UC10-4B9) and mAb to mouse IL-10 (JES5-16E3; all from eBioscience); and mAb to mouse CD4 (GK1.5), mAb to mouse IL-17A (TC11-18H10.1) and mAb to mouse Ki67 (B56; all from BD Bioscience). Biotinylated polyclonal antibody to mouse Nrp1 (BAF566) was from R&D Systems.

For intracellular staining of cytokines, lymphocytes from the LP were cultured for 6 h in complete medium (RPMI-1640 medium containing 10% FCS, 100 U/ml penicillin, 100 μg/ml streptomycin, 55 μM mercaptoethanol and 20 mM HEPES, pH 7.2) supplemented with 50 ng/ml PMA, 500 ng/ml ionomycin and GolgiPlug (BD Bioscience). The lymphocytes were then stained with mAb to CD3ε, mAb to CD4 and mAb to human CD2 (all identified above), followed by intracellular staining of interferon-γ, IL-17A, tumor-necrosis factor and IL-10 (antibodies identified above) with a Cytofix/Cytoperm kit (BD Bioscience). The stained samples were analyzed with a FACSCanto II or FACSAria II and with DIVA software (BD Biosciences) and FlowJo software, version 9.3.2 (Tomy Digital Biology).

***In vivo* EdU-incorporation assay.** For the detection of proliferating cells *in vivo*, GF and exGF mice received intraperitoneal injection of 3 mg EdU (5-ethynyl-2′-deoxyuridine) in 200 μl PBS, followed by administration of drinking water containing 0.8 mg/ml EdU for 2 d before the analysis. cLP cells that had incorporated EdU were visualized with a Click-it EdU Flow cytometry kit according to the manufacturer's instructions (Invitrogen).

Gene-expression profiling. Total RNA was extracted with TRIzol reagent (Life Technologies) according to a standard protocol and was subjected to microarray analysis with a GeneChip Mouse Genome 430 2.0 Array (Affymetrix). The data sets obtained were analyzed with GeneSpring GX 11 software (Agilent) and the Ingenuity pathway-analysis program (Ingenuity Systems).

Cell culture. CD3$^+$CD4$^+$CD44^{lo}CD62L^{hi} naive T cells were prepared from the spleen and lymph nodes by cell sorting as described above. Isolated naive CD4$^+$ T cells (5×10^5 cells per ml) were cultured for 3 d in complete RPMI-1640 medium supplemented with 5 ng/ml TGF-β and 10 ng/ml IL-2 (R&D Systems) and Dynabeads coated with mAb to CD3 and mAb to CD28 (Life Technologies) to induce differentiation into Foxp3$^+$ cells, then populations of differentiated cells were expanded up to an additional 4 d in the presence of 0.5 ng/ml TGF-β and 10 ng/ml IL-2. For cell-cycle analysis, induced T_{reg} cells were pulsed for 2 h with 10 μM EdU (Invitrogen). The cells were stained for EdU and 7-amino-actinomycin D with a Click-iT EdU flow cytometry kit before cell-cycle analysis with a FACSCanto II (BD) and FlowJo software, version 9.3.2 (Tomy Digital Biology).

***In vitro* suppression assays.** naive populations of CD3ε$^+$CD4$^+$hCD2$^+$ cells and CD3ε$^+$CD4$^+$CD62L^{hi}CD44^{lo} cells were purified as T_{reg} cells and responder cells, respectively, with the IMag Cell Separation System followed by cell sorting. For the preparation of antigen-presenting cells, splenocyte samples from C57BL/6J mice were depleted of Thy-1.2$^+$ cells and were irradiated with γ-irradiation (20 Gy). Responder cells labeled with carboxyfluorescein diacetate succinimidyl ester were cultured for 3 d together with T_{reg} cells at a ratio of 1:1 in the presence of antigen-presenting cells and mAb to CD3 (10 μg/ml; 145-2C11; eBioscience).

DNA-methylation analysis. Genomic DNA from CD3ε$^+$CD4$^+$hCD2$^+$ cells and CD3ε$^+$CD4$^+$hCD2$^-$ cells derived from mesenteric lymph nodes of male mice were extracted with an AllPrep DNA/RNA extraction kit (Qiagen), then were fragmented to approximately 200 base pairs by high-intensity focused ultrasound (Covaris) and were precipitated with histidine-tagged recombinant MBD1 ('methyl-CpG-binding-domain protein 1')[48]. After amplification by PCR, DNA fragments of the proper size were subjected to cluster generation and sequencing analysis with a HiSeq 1000 system (Illumina). Sequenced 'reads' were mapped to the mm9 assembly of the mouse genome (National Center for Biotechnology Information) with Bowtie software for the alignment of short DNA sequences. Peaks for each population were 'called' by model-based analysis of ChIP-seq data with a *P*-value threshold of less than 10^{-5}. The difference in methylation for a gene in one condition relative to its methylation in another condition was calculated with the normalized 'reads' mapped from 4 kilobases upstream to 4 kilobases downstream of its transcription start site. Transcription start sites were defined according to annotation on the Entrez database (National Center for Biotechnology Information).

Genomic bisulfite sequencing of the *Cdkn1a* promoter was done as described[17] with an EpiTect kit (Qiagen). The amplified fragments were cloned

doi:10.1038/ni.2886

with a TOPO TA cloning kit (Invitrogen) and were subsequently sequenced with the BigDye Terminator Cycle Sequencing system (Applied Biosystems) and an ABI PRISM 3100 Genetic Analyzer (Applied Biosystems). The PCR primers were designed with MethPrimer software (Li laboratory, Department of Urology, University of California, San Francisco). The sequences of the primer sets were as follows: 5′-ATATGTTGGTTTTTGAAGAGGG-3′ and 5′-ATCCCAAAAAATCCCACTATATC-3′.

Quantitative PCR. Total RNA was isolated from colonic tissues with an RNeasy mini kit (Qiagen) and was subjected to reverse transcription with a ReverTra Ace kit according to the manufacturer's instructions (Toyobo). The cDNA samples were amplified with a Thermal Cycler Dice Real Time System (TAKARA BIO), SYBR premix Ex Taq (TAKARA BIO) and the primer sets specific for mouse genes (sequences in **Supplementary Table 1**).

ChIP–quantitative PCR analysis. The MAGnify ChIP system (Life Technologies) was used as described[7], with a few modifications, for ChIP assays. Splenic $CD4^+CD25^+$ T cells were cultured for 3 d with Dynabeads Mouse T-Activator CD3-CD28 (Life Technologies) in the presence of 10 ng/ml IL-2 and 5 ng/ml TGF-β. The cells were allowed to 'rest' for 6 h in RPMI-1640 medium (Sigma-Aldrich) containing 0.1% FBS and then were stimulated for 1.5 h with or without 100 ng/ml IL-2. The cells were fixed for 10 min at 37 °C (in a water bath) with 1% formaldehyde, and the reaction was quenched by the addition of 125 mM glycine. Crude nuclei were isolated in SDS lysis buffer and were sonicated with a Microson (Misonix) and then a focused ultrasonicator (Covaris S220; Covaris) for the generation of chromatin fragments approximately 100–700 base pairs in length. The acoustic parameters were optimized as follows: duty cycle, 5%; intensity, 140 W; cycle and burst: 200 and 5 min. After evaluation of sample quality with an Agilent 2100 Bioanalyzer (Agilent), the sheared chromatin samples were immunoprecipitated overnight at 4 °C under gentle rotation with magnetic Protein A/G beads immobilized with anti-STAT5 (9363; Cell Signaling) or rabbit IgG (MAGnify ChIP kit; Life Technologies). After extensive washing of samples, immunocomplexes were eluted for 30 min at 55 °C, then were treated for 1 h at 65 °C with proteinase K for reversal of crosslinking. After extraction of DNA, quantitative PCR analysis was done with the following primer set specific for the promoter region of *Uhrf1*: 5′-TCCCTTTCTCCTCTCCCAGG-3′ and 5′-CTGCCGGCTATGCTCACTTT-3′.

Transfection of siRNA. Cells were transfect with siRNA through the use of an Amaxa Nucleofector kit according to the manufacturer's protocol (Ronza) with minor modifications. For this, 4 μg of negative control siRNA or pooled siRNA targeting *Cdkn1a* conjugated to the fluorescent dye Hilyte 488 (Nippon Gene) was added to Nucleofector solution containing 1×10^6 cells, followed by electroporation (Program: X-001). The cell cycle of cells containing Hilyte 488 was analyzed with Hoechst 33342, a cell-permeable DNA-binding dye, 24 h after electroporation. Transfection efficiency was approximately 10–15%. The sequence of the *Cdkn1a*-specific siRNA was as follows: 5′-GUUGCGCCGUGAUUGCGAU-3′, 5′-CCAGCCUGACAGAUUUCUA-3′ and 5′-GAACGGUGGAACUUUGACU-3′.

Immunoblot analysis. For immunoblot analysis, whole-cell extracts were prepared in RIPA lysis buffer containing a 'cocktail' of protease inhibitors (Nacalai Tesque). Equal amounts of cell lysate were separated by 5–20% gradient SDS-PAGE (Biorad). After transfer, proteins on Immobilon-P membranes (Millipore) were probed with the following primary antibodies: mAb to p21 (SX118; BD Pharmingen), mAb to GAPDH (6C5; Santa Cruz) and polyclonal antibody to Uhrf1 (M-132; Santa Cruz), together with horseradish peroxidase–conjugated antibody to mouse IgG (7076; Cell Signaling Technology) and antibody to rabbit IgG (7074; Cell Signaling Technology). The specific binding of the antibodies was visualized by an enhanced chemiluminescence detection system (Nacalai Tesque) and a LAS-3000 luminescent image analyzer (Fuji Film).

Histology. Prefixed colonic tissue sections were deparaffinized and rehydrated and were stained with either hematoxylin and eosin or Alcian blue–nuclear fast red. Specimens were histologically examined for the assignment of scores for the degree of colitis based on the following criteria: inflammatory infiltrates, mucosal hyperplasia and loss of goblet cells.

Adoptive-transfer experiments. Experimental colitis was induced in mice with deficient in recombination-activating gene 1 ($Rag1^{-/-}$) by adoptive transfer of $CD4^+CD25^-CD45RB^{hi}$ T cells as described[28]. Splenocyte samples fromC57BL/6 mice were enriched for $CD4^+$ T cells with the IMag Cell Separation System. The resultant $CD4^+$ T cells were labeled with fluorescein isothiocyanate–conjugated antibody to mouse CD3ε (145-2C11; BD Biosciences) and phycoerythrin-conjugated antibody to mouse CD45RB (16A; BD Biosciences), and $CD3\varepsilon^+CD4^+CD45RB^{hi}$ cells were isolated by sorting with a FACSAria II (BD Biosciences). The $Rag1^{-/-}$ recipients were given 1×10^5 $CD4^+CD25^-CD45RB^{hi}$ T cells via the tail vein and were analyzed at 6 weeks after transfer. For the experiment in **Supplementary Figure 6**, $CD4^+CD25^+$ T cells from $Uhrf1^{fl/fl}$*Cd4*-Cre or $CD4^{Cre}Uhrf1^{+/+}$ mice (8×10^4 cells per mouse) were transferred to $Rag1^{-/-}$ recipients together with $CD4^+CD25^-CD45RB^{hi}$ T cells from $CD45.1^+$ C57BL/6 mice (1×10^5 cells per mouse).

In the experiment in **Figure 7**, $CD4^+hCD2^+$ or $hCD2^-$ T cells from the spleen and peripheral lymph nodes of $Foxp3^{hCD2}$ mice (2×10^6 cells per mouse) were injected intravenously into 4- to 5-week-old $Uhrf1^{fl/fl}$*Cd4*-Cre$Foxp3^{hCD2}$ mice. The development of colitis in recipient mice was analyzed at 12 weeks of age.

Generation of mixed–bone marrow chimeras. Bone marrow cells isolated from femora of wild-type ($CD45.1^+$; 1×10^6 cells per mouse) and $Uhrf1^{fl/fl}$ *Cd4*-Cre or $Uhrf1^{+/+}$*Cd4*-Cre mice ($CD45.2^+$; 1×10^7 cells per mouse) were injected intravenously into $Rag1^{-/-}$ mice treated with γ-irradiation (8 Gy) before the injection. Six weeks later, the cLP of the recipient mice was analyzed by flow cytometry.

Immunofluorescence staining. Immunofluorescence staining of cross-sections of colonic tissues was done as described[49].

Statistical analysis. Differences between two or more groups were analyzed by Student's *t*-test or one-way ANOVA followed by Tukey's test. When variances were not homogeneous, the data were analyzed by the nonparametrical Mann-Whitney *U*-test or the Kruskal-Wallis test followed by the Scheffé test.

46. Weigmann, B. *et al.* Isolation and subsequent analysis of murine lamina propria mononuclear cells from colonic tissue. *Nat. Protoc.* **2**, 2307–2311 (2007).
47. Yamaguchi, T. *et al.* Control of immune responses by antigen-specific regulatory T cells expressing the folate receptor. *Immunity* **27**, 145–159 (2007).
48. Morita, S. *et al.* Genome-wide analysis of DNA methylation and expression of microRNAs in breast cancer cells. *Int. J. Mol. Sci.* **13**, 8259–8272 (2012).
49. Obata, Y. *et al.* Epithelial cell-intrinsic Notch signaling plays an essential role in the maintenance of gut immune homeostasis. *J. Immunol.* **188**, 2427–2436 (2012).

SCIENTIFIC REPORTS

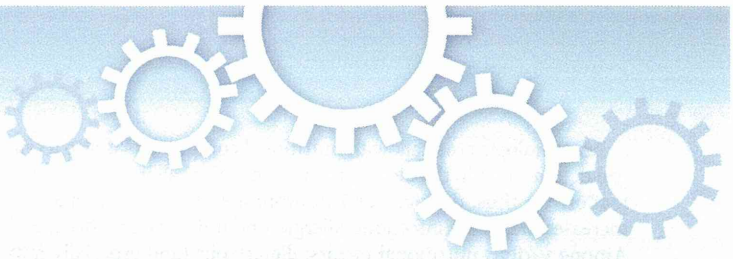

OPEN

SUBJECT AREAS:
MUCOSAL IMMUNOLOGY
IMMUNOSUPPRESSION

Received
26 September 2014

Accepted
16 February 2015

Published
7 April 2015

Correspondence and requests for materials should be addressed to J.K. (kunisawa@nibio.go.jp) or M.A. (makoto.arita@riken.jp)

Dietary ω3 fatty acid exerts anti-allergic effect through the conversion to 17,18-epoxyeicosatetraenoic acid in the gut

Jun Kunisawa[1,2,3,4,5,6], Makoto Arita[7,8,9,10], Takahiro Hayasaka[11], Takashi Harada[11], Ryo Iwamoto[9], Risa Nagasawa[1,2], Shiori Shikata[1,2], Takahiro Nagatake[1], Hidehiko Suzuki[1], Eri Hashimoto[1,2], Yosuke Kurashima[1,2], Yuji Suzuki[2], Hiroyuki Arai[4,9], Mitsutoshi Setou[11,12] & Hiroshi Kiyono[2,3,4,13,14]

[1]Laboratory of Vaccine Materials, National Institute of Biomedical Innovation, Osaka 567-0085, Japan, [2]Division of Mucosal Immunology, Department of Microbiology and Immunology, The Institute of Medical Science, The University of Tokyo, Tokyo 108-8639, Japan, [3]International Research and Development Center for Mucosal Vaccines, Institute of Medical Science, The University of Tokyo, Tokyo, Japan, [4]Core Research for Evolutional Science and Technology (CREST), Japan Science and Technology Agency, Tokyo 102-0075, Japan, [5]Kobe University Graduate School of Medicine, Hyogo 650-0017, Japan, [6]Graduate School of Dentistry and Graduate School of Pharmaceutical Sciences, Osaka University, Osaka 565-0871, Japan, [7]Laboratory for Metabolomics, RIKEN Center for Integrative Medical Sciences, Kanagawa 230-0045, Japan, [8]Graduate School of Medical Life Science, Yokohama City University, Kanagawa 230-0045, Japan, [9]Departments of Health Chemistry, Graduate School of Pharmaceutical Sciences, The University of Tokyo, Tokyo 113-0033, Japan, [10]Precursory Research for Embryonic Science and Technology (PRESTO), Japan Science and Technology Agency (JST), Tokyo 102-8666, Japan, [11]Department of Cell Biology and Anatomy, Hamamatsu University School of Medicine, Shizuoka 431-3192, Japan, [12]The Institute of Medical Science, The University of Tokyo, Tokyo 108-8639, Japan, [13]Department of Medical Genome Science, Graduate School of Frontier Science, The University of Tokyo, Chiba 277-8562, Japan, [14]Graduate School of Medicine, The University of Tokyo, Tokyo 113-0033, Japan.

ω3 polyunsaturated fatty acids (PUFAs) have anti-allergic and anti-inflammatory properties, but the immune-metabolic progression from dietary oil remains to be investigated. Here we identified 17,18-epoxyeicostetraenoic acid (17,18-EpETE) as an anti-allergy metabolite generated in the gut from dietary ω3 α-linolenic acid (ALA). Biochemical and imaging mass spectrometry analyses revealed increased ALA and its metabolites, especially eicosapentaenoic acid (EPA), in the intestines of mice receiving ALA-rich linseed oil (Lin-mice). In murine food allergy model, the decreased incidence of allergic diarrhea in Lin-mice was due to impairment of mast cell degranulation without affecting allergen-specific serum IgE. Liquid chromatography–tandem mass spectrometry-based mediator lipidomics identified 17,18-EpETE as a major ω3 EPA-derived metabolite generated from dietary ALA in the gut, and 17,18-EpETE exhibits anti-allergic function when administered *in vivo*. These findings suggest that metabolizing dietary ω3 PUFAs generates 17,18-EpETE, which is an endogenous anti-allergic metabolite and potentially is a therapeutic target to control intestinal allergies.

Food allergies affect the quality of life of patients and their families; they may even cause severe or fatal reactions. Although the prevalence of food allergy has increased recently, current standards of care remain focused on the elimination of dietary allergens because available means of prevention and treatment are inadequate[1]. The immunologic mechanisms in the development of food allergy involve the disruption of oral tolerance, induction of Th2-type responses, allergen-specific IgE production, and mast cell (MC) activation[2,3]. These immune responses have been studied in several murine models of food allergy (including ours)[4–8]. Using egg white ovalbumin (OVA) as a model food allergen, we induce allergic diarrhea in mice accompanied by aberrant Th2-type responses, increased OVA-specific serum IgE, and MC infiltration and degranulation in the large intestine[4]; this type I intestinal allergy is therefore similar to that of human patients with egg food allergy. Our subsequent study shows that the development of intestinal allergy is mediated by sphingosine 1-phosphate by controlling the trafficking of pathogenic cells, such as Th2 cells and MCs[9]. Therefore, various host-derived factors (e.g., cytokines, antibodies, and lipid mediators) are likely involved in the development of intestinal allergy.